

# Fizeau Confocal Laser Scanning Interference Microscope

P. F. Meilán and M. Garavaglia

Departamento de Física, Facultad de Ciencias Exactas,  
Universidad Nacional de La Plata

and

Laboratorio de Procesamiento Láser, Centro de Investigaciones Ópticas (CIOp)

Mail address: CIOp, CC 124, Correo Central, 1900 La Plata, Argentina

E-Mail: pfmeilan@odin.ciop.unlp.edu.ar

Recebido em 18 de maio 1998

In this paper, Fizeau interferometry is introduced in conjunction with confocal laser scanning microscope as a new interferential method. In this preliminary investigation interference fringes formation was studied. A theoretical model of the method is presented and a comparative analysis with the experimental and theoretical results was performed.

## I Introduction

The Confocal Laser Scanning Microscopy (CLSM) is a powerful imaging technique capable of obtaining 3D images from various objects through a high-resolution optical tomography procedure. However, the possibility of introducing interferometric observations remarkably enhances the optical tomography capabilities of the CLSM.

In fact, the interferometric observation allows measurement of the optical signals phase and amplitude increasing the ability of the CLSM to determine the objects surface profile variations or phase shifts caused by translucent or transparent objects.

Other combinations of CLSM and interferometric techniques have been reported in the literature. These include the use of both Michelson and Mach-Zehnder interferometers together with CLSM [1, 2, 3]. In addition, fiber optic illumination devices have been also introduced [4].

In this paper, the introduction of the Fizeau interferometric technique to the CLSM is described. This method is very simple and assures the observation of very high contrast interference fringes. To obtain these fringes, it is necessary to put a coverglass at the top of

the sample holder slide forming a small angle with it as illustrated in Fig.1. In this way, the Fizeau fringes resulting from the reflection on the slide first surface overlap with the ones formed among the object, slide and coverglass surface.

With this method, surfaces topography can be analyzed. The Fizeau fringes technique allows the observation of surface fringes, which characterize its topography, particularly in case of liquids and solids that strongly absorb at the observation wavelength.

## II Theory

In this section the interference pattern formed between two reflected wavefronts on the mirror  $M$  and coverglass  $SM$ , according to the Fizeau interferometer arrangement, will be studied. In Fig.1 the interferometric system is shown. The coverglass refractive index and thickness are known. In this case the sample object is the mirror  $M$  itself.

In this study, the axial response profile  $V(z)$  will be considered. The axial complex amplitude distribution  $V(z)$  can be written, for a free aberration aplanatic system, which obeys the *sine condition*, as [5]:

$$V(z) = \exp\left(\frac{iu}{2} \cot^2 \frac{\alpha}{2}\right) \left[ \frac{\sin(u/2)}{u/2} + i \frac{\tan^2(\alpha/2)}{u/2} \left( \frac{\sin(u/2)}{u/2} - \cos(u/2) \right) \right] \quad (1)$$

where  $\sin\alpha$  is the objective numerical aperture and  $u$  is the adimensional axial coordinate defined as  $u = 4kz\sin^2(\alpha/2)$ , and  $k = 2\pi/\lambda$ . In practice, the photodetectors only allow measuring the axial response irradiance given by  $|V(z)|^2$ . If the  $V(z)$  distribution evaluated on  $SM$  is denoted by  $V_{SM}$  and on  $M$  by  $V_M$ , it is possible to write the irradiance distribution as:

$$I = |r_{SM}V_{SM} + r_M V_M|^2, \quad (2)$$

where  $r_M$  is the Fresnel's reflection coefficient of the plane mirror  $M$  and  $r_{SM}$  of the coverglass  $SM$ . Both coefficients can be written as [6]:

$$r_{SM,M} = \frac{(r_{\parallel} + r_{\perp})}{2}, \quad (3)$$

where:

$$r_{\parallel} = \frac{-n_2 \cos\theta_1 + n_1 \cos\theta_2}{n_2 \cos\theta_1 + n_1 \cos\theta_2}, \quad \text{and} \quad r_{\perp} = \frac{n_1 \cos\theta_1 - n_2 \cos\theta_2}{n_1 \cos\theta_1 + n_2 \cos\theta_2}. \quad (4)$$

A convenient form to write the reflected fields is:

$$V_{SM} = |V_{SM}|e^{i\delta_{SM}}, \quad V_M = |V_M|e^{i\delta_M}. \quad (5)$$

Then, rewriting expression (2) as:

$$I = I_{SM} + I_M + J_{SM,M}, \quad (6)$$

and taking into account that the reflected fields have the same polarization state, it is possible to write the term in (6) as follows:

$$I_{SM} = \frac{|r_{SM}V_{SM}|^2}{2}, \quad I_M = \frac{|r_M V_M|^2}{2}, \quad (7)$$

$$J_{SM,M} = \frac{r_{SM}r_M}{2}(V_{SM}V_M^* + V_{SM}^*V_M). \quad (8)$$

Introducing (5) into (8),  $J_{SM,M}$  results:

$$J_{SM,M} = r_{SM}r_M|V_{SM}||V_M|\cos\delta, \quad (9)$$

where  $\delta = |\delta_{SM} - \delta_M| = n_f \beta x (4\pi/\lambda_0)$  according to the Fizeau interferometer description [7], where  $\beta$  is the wedge angle,  $n_f$  is de surrounding refractive index and  $x$  is the field interferential coordinate transverse to the fringes. Here it is assumed that  $r_M = 1$  and  $r_{SM} = (n_f - 1)/(n_f + 1)$ , for simplicity.

In a confocal microscope, an image is created at a given axial  $z$  position by scanning in the  $x - y$  plane.

In the geometry given in Fig.1, the electric field amplitude on the  $SM$  is an  $x$  dependent function, while the electric field on the plane mirror  $M$  is constant.

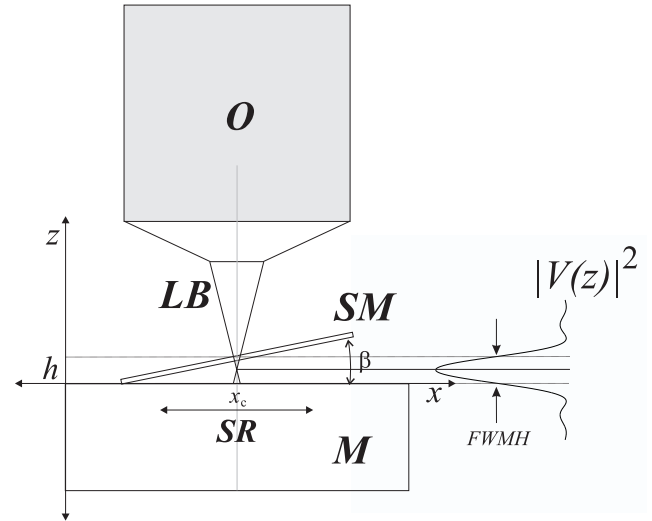


Figure 1. This figure shows the experimental setup where  $O$  is a 10X magnification objective with 0.3 NA,  $LB$  the laser beam,  $M$  the mirror,  $SM$  the coverglass and  $|V(z)|^2$  the square modulus of the axial response profile having a width FWHM. The scanning region  $SR$  is centered at  $x = x_c$ , where  $h$  is the vertical local height between  $M$  and  $SM$  for an angle  $\beta$ .

After introducing equations (9) and (??) into (6) and knowing that  $\lambda_0 = 568$  nm,  $n_f = 1$  and  $n = 1.51$ , it is possible to calculate the intensity distribution profile for two cases: (a)  $\beta = 14.4897 \pm 0.0001$  mrad, (b)

$\beta = 38.904 \pm 0.002$  mrad. Both computed simulations are show in Fig.2.

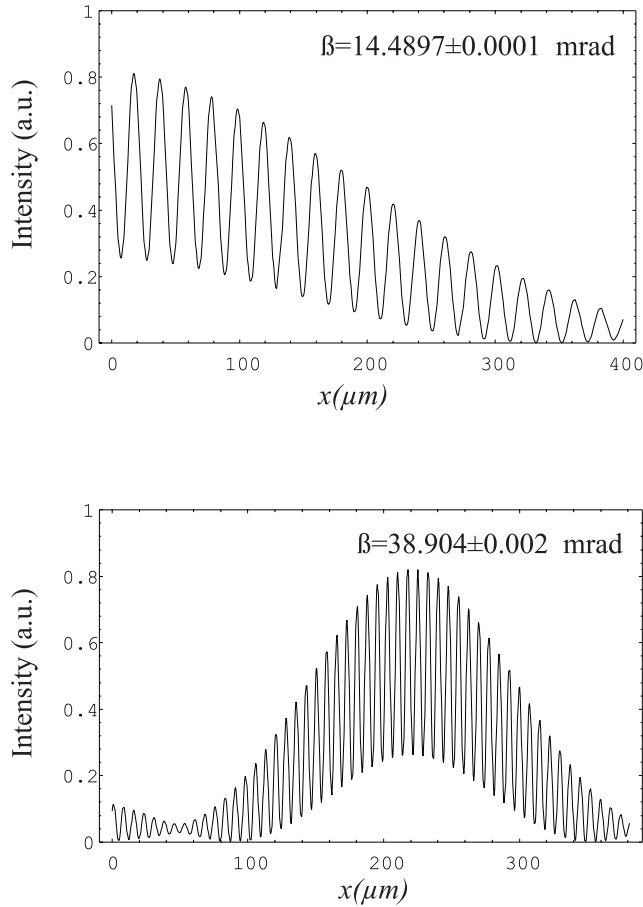


Figure 2. Interferometric pattern profile obtained by computing simulation for tow cases: a)  $\beta = 14.4897 \pm 0.0001$  mrad and b)  $\beta = 38.904 \pm 0.002$  mrad.

As it is well known the width of the axial irradiance distribution  $|V(z)|^2$  depends from  $\lambda$ , the numerical aperture ( $NA$ ) of the microscope objetive and the diameter of the pinhole placed in front of the photodetector ( $D$ )[8]. Then, if for a given  $NA$  objetive the  $FWHM$  varies with  $D$ , the expressions of  $I_{SM}$ ,  $I_M$  and  $J_{SM,M}$  will notably change according with the vertical local height  $h$  mesured between the mirror  $M$  and the coverglass  $SM$ , or, in another words, they will change as a function of the scanning position  $x$  through the wedge experimental angle  $\beta$ . One aspect of this fact was analyzed previously in this section. It is that related with the generation of the interferential fringes themselves.

Formally speaking, densitometric traces allows to compute the visibility of Fizeau interferential fringes point to point. According with the Michelson definition of the visibility  $\mathcal{V}$ , the best observation of fringes

will be performed when the maximun and minimun values of the irradiance  $I$  at equation (6) reach  $I_{Max} = 4I_0$  for  $\delta = 2m\pi$  and  $I_{min} = 0$   $\delta = (2m + 1)\pi$ , assuming that  $I_M = I_{SM} = I_0$ .

But a new aspect arises when interferential fringes must be observed at the highest sectioning capacity of the CLSM. The main function of the pinhole placed in front of the photodetector is to contribute to the sectioning of the object response along the  $z$ -axis. Then, highest sectioning capacity in Fizeau interferometry using CLSM could avoid the observation of fringes. In fact, if the  $FWHM$  of the  $|V(z)|^2$  is smaller than the vertical local height  $h$  between the mirror  $M$  and the coverglass  $SM$  at a certain position  $x = x_1$ , means that  $V_{SM}$  can reaches a significant value when the coverglass  $SM$  is at focus, while  $V_M$  is negligible or small on the mirror  $M$ . In this case, the equation (6) is equal to the expresion of  $I_{SM}$ :

$$I = I_{SM} + I_M + J_{SM,M} = I_{SM}, \quad (10)$$

which is the image of the coverglass at the position  $x = x_1$ . In the opposite case, when the mirror  $M$  is at focus, equation (6) results in:

$$I = I_{SM} + I_M + J_{SM,M} = I_M, \quad (11)$$

which is the image of the mirror  $M$ . In both cases the interferential term  $J_{SM,M} = 0$ , and the fringes visibility  $\mathcal{V}(x_1) = 0$ . So, the visibility  $\mathcal{V}(x)$  depends from the numerical aperture  $NA$  of the microscope objective, the pinhole diameter  $D$  and the angle  $\beta$  formed by the mirror  $M$  and the coverglass  $SM$ . By introducing the value of  $J_{SM,M}$  given by equation (9) in the expression (6) it is possible to derive a visibility equation according to the Michelson definition. Equation (12) gives the mathematical support to the visibility dependence on the lateral  $x$  coordinate:

$$\mathcal{V}(x) = \frac{J_{SM,M}(x)/\cos\delta}{I_{SM}(x) + I_M(x)} \quad (12)$$

and Fig.3 represents it in a normalized fashion for a typical axial  $z$  position.

### III Experimental results

By using the experimental setup showed in Fig.1, two interference patterns corresponding to the same cases

simulated in Fig.2 were obtained. They are depicted at Fig.4. It shows the picture of experimental results and their densitometric profiles when the FWHM of the

$V(z)$  distribution is equal to the vertical local height  $h$  of the wedge at the central point  $x_c$  of the scanning region.

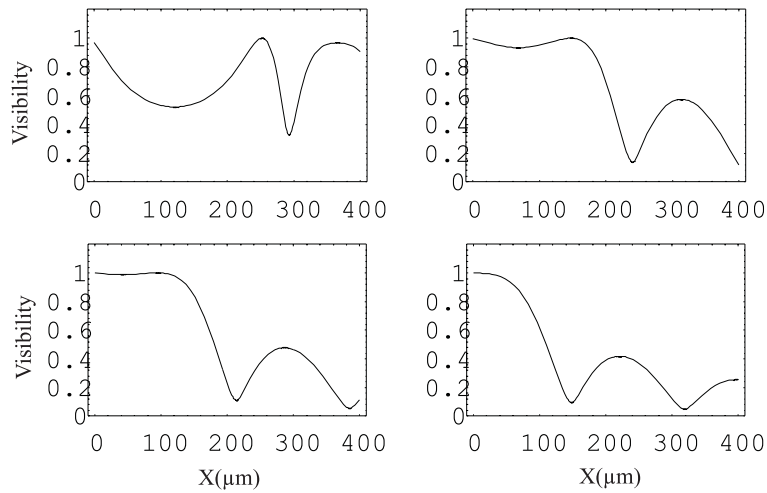


Figure 3. Simulated normalized visibility curve calculated with equation (12) corresponding to the experimental Fizeau interference fringes showed at Figure 5 c).

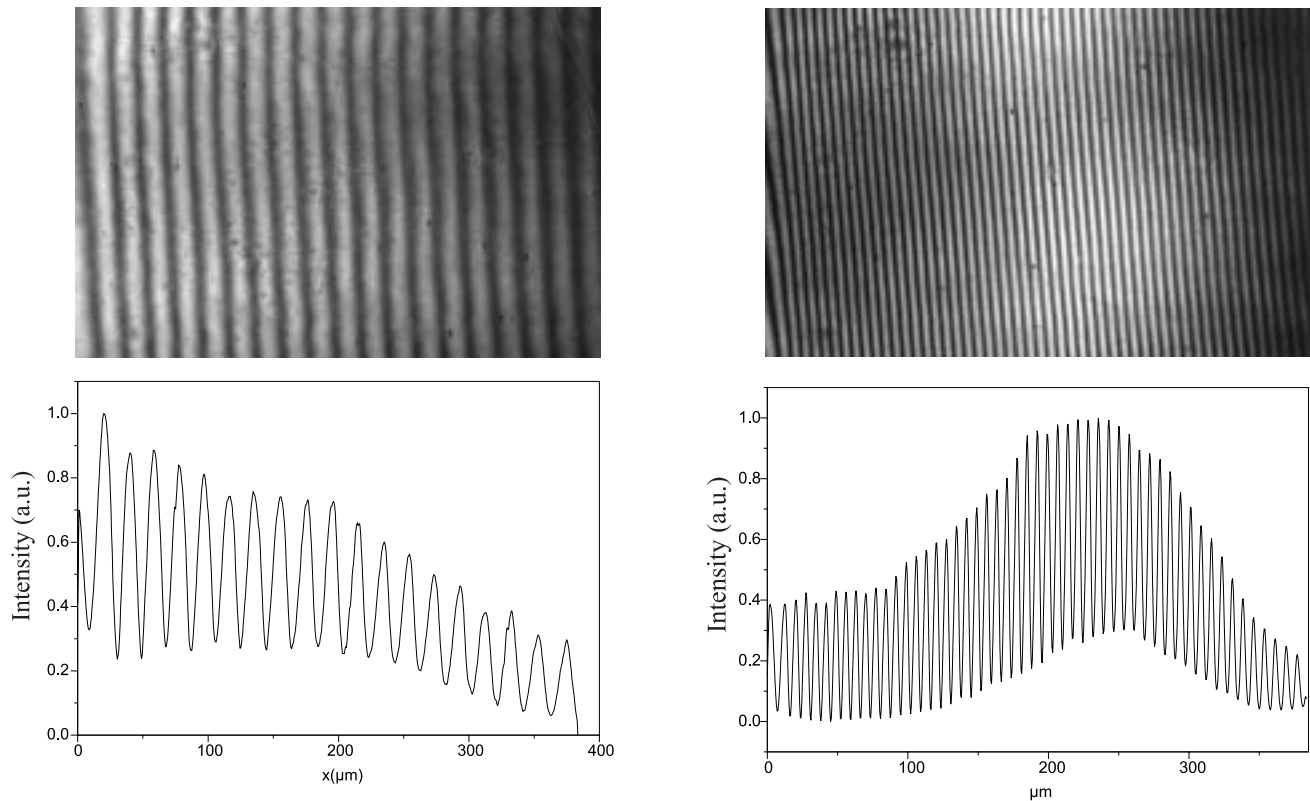


Figure 4. Interferometric patterns obtained with a confocal laser scanning microscope and their densitometric profiles. a)  $\beta = 14.4897 \pm 0.0001$  mrad and b)  $\beta = 38.904 \pm 0.002$  mrad.

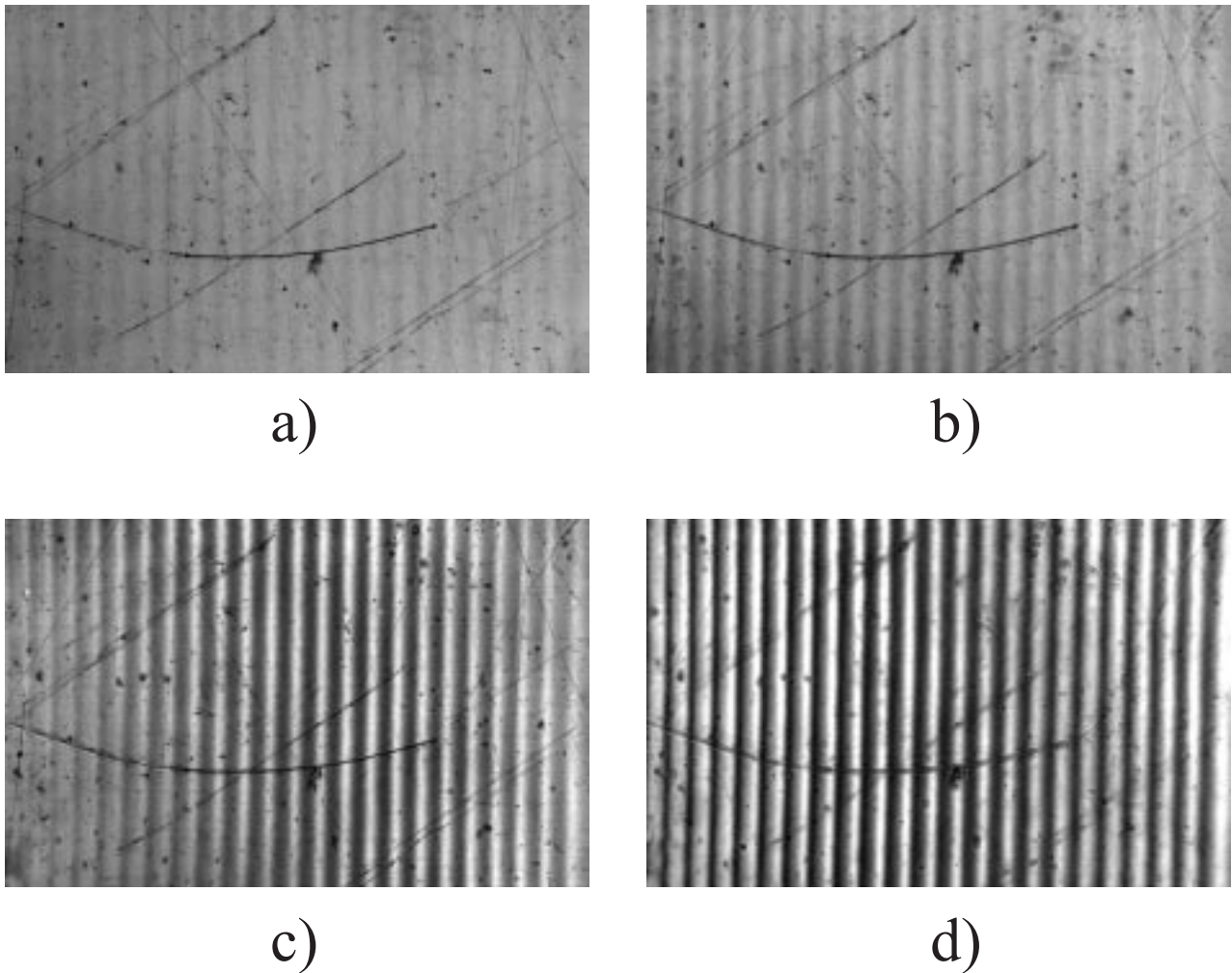


Figure 5. Fizeau interference fringes at four CLSM focus for the wedge angle  $\beta = 38.9$  mrad. (For details see the text).

In a similar experiment to that described before which was performed to get interferential fringes at different values of  $\beta$ , interference was observed exclusively varying the focus of the microscope keeping the other instrumental variables fixed. Fig.5 shows four pictures of the Fizeau interferential fringes as a function of the focus for the wedge angle  $\beta = 38.9$  mrad. The microscope was sequentially focused at four levels: **a)** near the mirror  $M$  surface, **b)** and **c)** at two different steps from the mirror  $M$  and **d)** near the  $SM$  coverglass.

The Fizeau interferential fringes in the picture **a)** showed at Fig.5, closely corresponds to the visibility calculated using equation (12) and depicted in Fig.3.

## IV Conclusions

Excellent agreement was observed between experimental results and theoretical predictions. This indicates

that this new interferometric method shows promise for increasing the axial resolution of the confocal microscope. The Fizeau interferometer is a very simple device and it is possible to apply it to any confocal microscope.

Because of its properties, this method is very convenient to study the surface profiles of droplets and their temporal evolution. Fig.6 shows four interferential images of the temporal evolution of an oil droplets spaced 40 minutes from one to the next.

Besides, in case that the sample under CLSM inspection strongly absorbs at the employed wavelength, the Fizeau confocal laser scanning interference microscopy can be applied without disturbing its surface. As an example of disturbed surface Fig.7 shows the effect of CLSM on photographic film, which was cratered in the two points under CLSM observation.

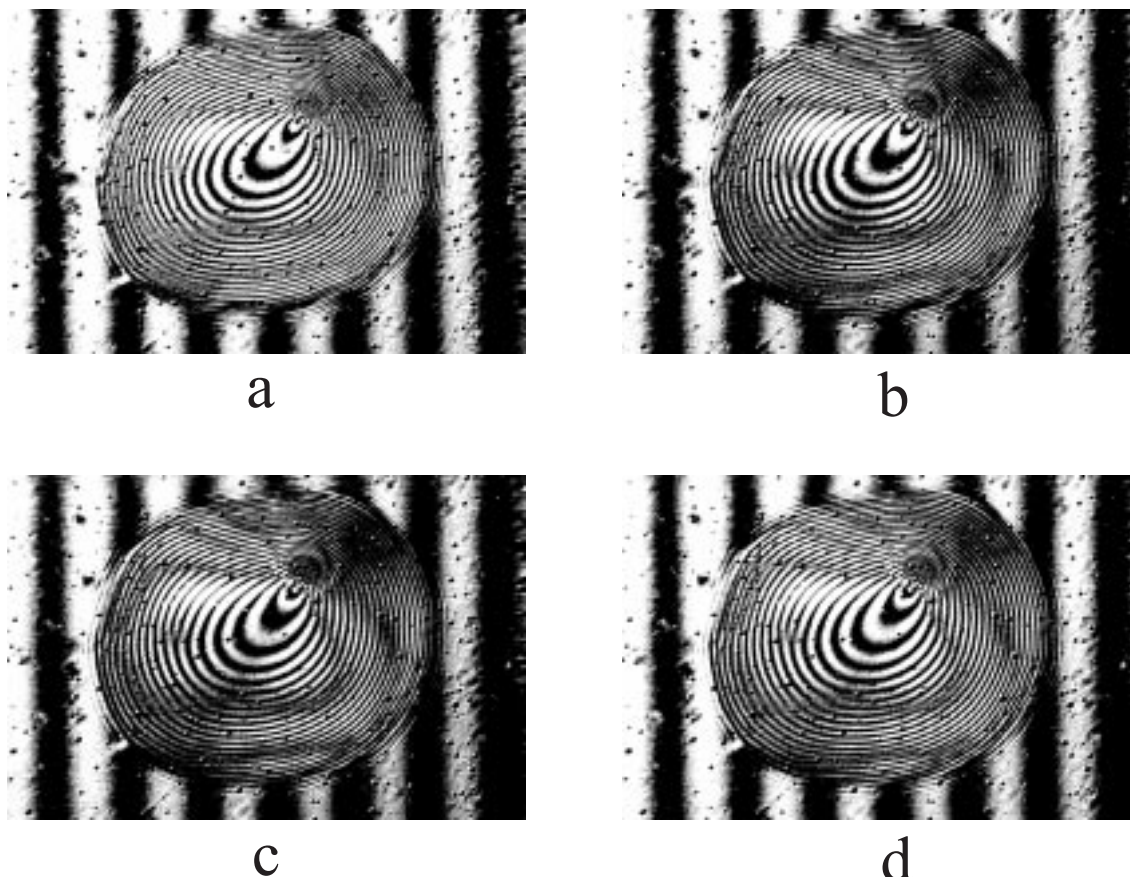


Figure 6. Time evolution of an oil droplets. a) Initial time  $t=0$ , b)  $t=40$  minutes, c)  $t=80$  minutes and d)  $t=120$  minutes (2 hours).

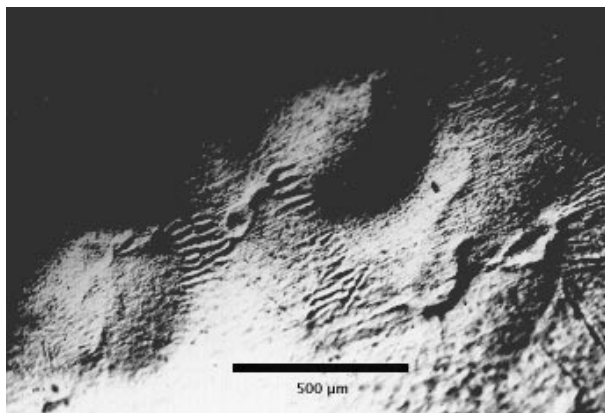


Figure 7. Photographic film damage produced by CLSM observation.

## V Acknowledgements

Authors acknowledge the fruitful discussions with Prof. Dr. C. J. R. Sheppard during his stay at CIOP as International Commission for Optics Traveling Lecturer (September 1997), and to the Instituto de Neurobiología, Buenos Aires, Argentina.

This work was partially financed by the Consejo Nacional de Investigaciones Científicas y Técnicas (CONICET), Argentina, the Universidad Nacional de La Plata (UNLP), and the Comisión de Investigaciones Científicas (CIC) de la Provincia de Buenos Aires, Argentina. P. F. Meilán is indebted to CIC for his Research and Training Fellowships.

## References

- [1] D.K. Hamilton and C.J.R. Sheppard, "A confocal interference microscope", *Opt. Acta* **29**, 1573 (1982).
- [2] C.J.R. Sheppard and Yunrui Gong, "Improvement in axial resolution by interference confocal microscopy", *Optik* **87**, 129 (1991).
- [3] H. Zhou, M. Gu and C.J.R. Sheppard, "Confocal interference microscopy: a difference between dry and immersion lenses", *Optik* **97**, 94 (1994).
- [4] M. Gu and C.J.R. Sheppard, "Fiber-optical confocal scanning interference microscopy", *Opt. Comm.* **100**, 79 (1993).
- [5] C.J.R. Sheppard and T. Wilson, "Effects of high angles of convergence on  $V(z)$  in de scanning acoustic microscope", *Appl. Phys. Lett* **38**, 858 (1981).

- [6] C.J.R. Sheppard and M. Gu, "Axial imaging through an aberrating layer of water in confocal microscopy", *Opt. Comm.* **88**, 180 (1992).
- [7] M. Born and E. Wolf, "Principles of optics", pp. 286-287, 2nd Ed. Pergamon Press (1964).
- [8] T. Wilson and A. R. Carlini, "Size of the detector in confocal imaging system", *Opt. Lett.* **12**, 227-229 (1987).

